

PHOTOEMISSION FROM COATED SURFACES: COMPARISON OF THEORY TO EXPERIMENT

K. L. Jensen, Naval Research Laboratory, Washington DC, USA
D. W. Feldman, N. Moody, P. G. O'Shea, U. of Maryland, College Park, MD, USA
A. Balter, Oglethorpe University, Atlanta, GA, USA

Abstract

A comparison of a theoretical photoemission model with experimental measurements of the quantum efficiency (QE) of Tungsten (and Silver) coated with Cesium as a function of coverage and incident laser wavelength are made. The theory uses models of the work function reduction due to Cesium on bulk metals using Gyftopoulos-Levine theory, changes in the probability of emission due to scattering, a modified Fowler-Dubridge estimate of the probability of emission as a function of material parameters, and a quantum mechanical reflection factor. The agreement between theory and experiment for Cs on W is excellent. A recent study of Cs on Ag is shown and discussed.

INTRODUCTION

Photocathodes are critical components in photoinjectors for high power free electron lasers (FEL's), energy-recovery linac (ERL) driven x-ray sources, high energy linear colliders, and other applications that require laser-switched sources of prebunched electron beams [1, 2, 3, 4, 5]. We report on experiments and theoretical models conducted with the goal of developing a custom-engineered rugged, self rejuvenating photocathode with high quantum efficiency (QE) using the longest wavelength drive laser for, in particular, RF photoinjectors for high power FEL's and accelerators. We have elsewhere evaluated the performance of dispenser cathodes as photoemitters [6], and their usage has shown promise [7, 8]. In addition to the pressing need for suitable photocathodes, there is also a need for the development of photoemission models validated by experiment from coated metals suitable for use by beam simulation codes to model the impact of emission non-uniformity and emittance growth [9, 10, 11]. The models must account for effects of laser heating, thermal evolution, surface conditions, laser parameters, material characteristics, and include components dedicated to coverage non-uniformity & field enhancement. We discuss the status of those models and compare their performance to experimental results for Cesium (Cs) on bulk metals such as Tungsten (W) and Silver (Ag).

Quantum efficiency (QE) is the ratio of number of ejected electrons per incident (not absorbed) photon, and, when the photon energy is above the work function so that the emission bunch has the same pulse width as the incident laser pulse, a common formula is

$$QE = \frac{\hbar\omega}{q} \left(\frac{J_e}{I_\lambda} \right) = 1.2398 \frac{J_e [A/cm^2]}{I_\lambda [W/cm^2] \lambda [\mu m]} \quad [1]$$

where $\hbar\omega$ is the photon energy, q is the electron charge, I_λ is the laser intensity, and J_e is the emission current. In the present work, we have moved beyond the approximations inherent in Eq. [1] and now evaluate QE using a time-dependent simulation code to monitor electron temperature as a function of time-dependent laser intensity, as all factors (save the reflectivity at present) are temperature-dependent. Thus, a time dependent temperature necessitates rewriting QE as

$$QE = \frac{\hbar\omega}{q} \frac{\int_{-\infty}^{\infty} J(F, T(t)) dt}{\int_{-\infty}^{\infty} I_\lambda(t) dt} \quad [2]$$

We have shown elsewhere [12] that

$$J_e(t) \approx \frac{q(1-R)}{2\hbar\omega} I_\lambda(t) \frac{U[\beta(\hbar\omega - \phi)]}{U[\beta\mu]} G\left(\frac{m\delta}{\hbar k_v \tau}\right) \quad [3]$$

where R is the reflectivity of the surface, $G/2$ is the fraction of electrons surviving scattering events after photoexcitation on their journey to the surface, and the U function ratio accounts for the probability the photoexcited electrons can overcome the surface barrier (it is an extension of the widely used Fowler-Dubridge model). Further, δ is the laser penetration depth, m is the electron mass, $\hbar^2 k_v^2 / 2m = \mu + \phi$, β is the inverse temperature $1/k_B T(t)$, and ϕ is the height of the surface barrier above the chemical potential μ (or Fermi level) and is $\phi = \Phi - \sqrt{4QF}$, where Φ is the work function, F is the product of q with applied field, and $Q = 0.36$ eV-nm. Note, first, that the Fowler-Dubridge factor is explicitly temperature-dependent, whereas the scattering factor is implicitly through the dependence of the femtosecond-scale relaxation time on electron (and lattice) temperature. Integral forms of U and G are

$$U(x) = \int_{-\infty}^x \ln(1 + e^y) dy \quad [4]$$

$$G(x) = \frac{2}{\pi} \int_0^{\pi/2} \frac{\cos(\theta)}{\cos(\theta) + x} d\theta$$

The electron and lattice temperatures are related through coupled differential equations relating absorbed power to heat diffusion near the surface, and the methods to calculate them are protracted [13]. Given the complex interdependence of all factors on temperature, approximations for Eq. [2] are good only for special circumstances: in all calculations below designated as "numerical simulation" we

therefore evaluate Eq. [2] in the manner detailed in Refs. [12] and [13], in which the temperature is obtained by numerically solving the coupled partial differential equations relating electron and lattice temperatures, and material dependent properties are computed or extrapolated from the literature.

Temperature Rise due to Laser Intensity

A rough estimate of the temperature rise due to the incident laser can be made by assuming that the total laser energy is uniformly distributed over a slab of thickness L and that the lattice and electron temperature are equal. These approximations simplify the coupled partial differential equations to be

$$\Delta T \approx (\Delta E / L) / \{C_e(T_o) + C_l(T_o)\} \quad [5]$$

where the C_e and C_l are specific heats of the electron gas and the lattice, and ΔE is the *absorbed* energy per unit area from the laser. It is useful to use the room temperature and asymptotic values of the specific heats for the electron and lattice, respectively.

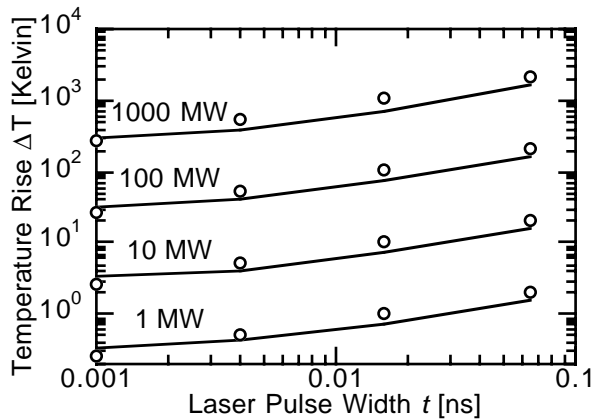


Figure 1: Comparison of Eq. [5] (circles) with numerical simulation for Cu and an incident wavelength of 266 nm.

The width of the slab is estimated by taking it as the full width at half maximum value of the Gaussian-like expanding temperature profile: from the heat diffusion equation, the form of L should therefore be $L = \delta\sqrt{t/t_o}$, where δ is the laser penetration depth and t_o is a time parameter that must be determined by other means: if we evaluate it for a given pulse length using numerical simulation, then we have found that Eq. [5] is a reasonably good (but not adequate for comparisons to experiment) estimate of the temperature rise for other pulse widths (t). A comparison of Eq. [5] with numerical simulation in the case of copper parameters is shown in Figure [1] to give an indication of how temperature rises

scale with laser intensity and pulse duration, copper being chosen because it is a common photocathode material and experimental results are obtainable [14, 15].

Coverage Dependent Work Function

The model of Gyftopoulos and Levine was used to determine the work function depending on the fractional monolayer coverage of the surface [16]: the coverage θ is the fraction of a monolayer present on the surface, and is assumed to be uniformly distributed. For submonolayers, $\theta < 1$. Compared to past work [5], some modifications have been made. The work function is evaluated according to

$$\Phi(\theta) = \phi_f - (\phi_f - \phi_m)\theta^2(3 - 2\theta)\{1 - G(\theta)\} \quad [6]$$

$$G(\theta) = \frac{\left(\frac{r_o}{r_c}\right)^2 \left(1 - \frac{2}{w} \left(\frac{r_w}{R}\right)^2\right)}{\left(1 + n \left(\frac{r_c}{R}\right)^3\right) \left(1 + \frac{9n}{8} (f\theta)^{3/2}\right)} f\theta$$

where ϕ_f and ϕ_m are monolayer and bare work functions, respectively, r_c and r_w are the covalent radii of the cover (*e.g.*, Cs) and bulk (*e.g.*, W) atoms, $n = 1$ for Cs and 1.65 for Ba, f is the number of C atoms per an area $(2r_c)^2$, and $w = n_f f (r_w/r_c)^2$ where $n_f = 4$ for Cs on W, Mo, and Ta but 2 for Ba, Sr, Th on W, *etc.* f is determined by that value which brings various experimental measurements [17] into agreement via a least-squares analysis, as shown in Figure 2, a procedure described elsewhere [13]. For Cs on W, $f = 1.088$ is optimal.

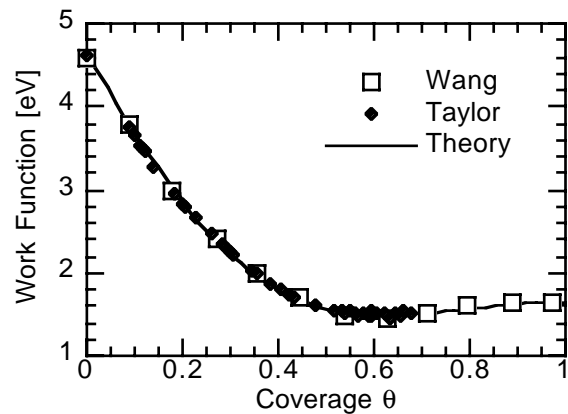
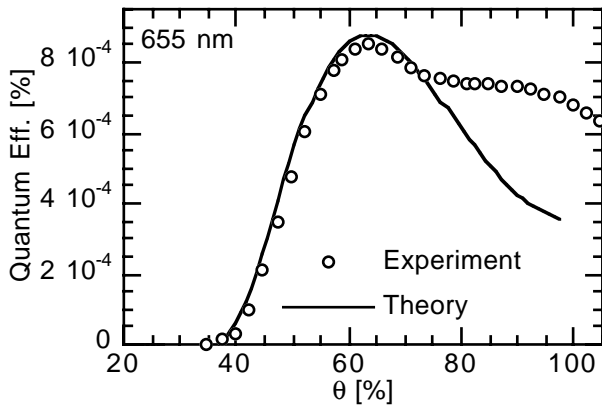
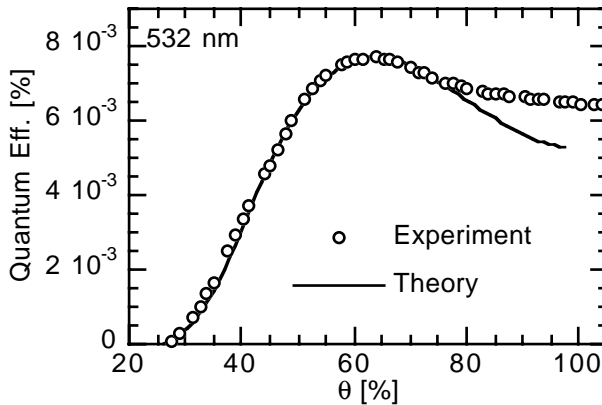
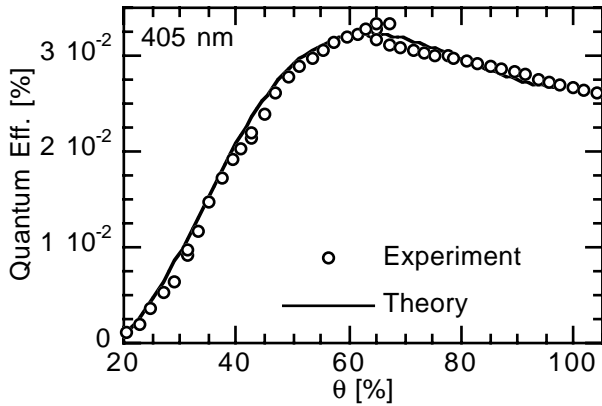


Figure 2: Comparison of Eq. [6] with the data of Wang and Taylor, *et al.* (Ref. 17).

Relation of Theory to Experiment

The aforementioned theory was used to analyze experimental evaluations of QE for Cs on W for incident wavelengths of 407, 532, and 655 nm. Care is taken to insure that the laser is focused only on the cathode: because Cs atoms are deposited throughout the chamber and not just on the cathode surface, stray laser light could cause photoemission if incident on any other metallic components. Current measurements were performed

during Cs evaporation, so a screen held at negative with respect to ground is placed in front of the sources (held at ground) to ensure that only neutral Cs arrives at the cathode surface by repelling ionized Cs. The amount of Cs evaporated on the W surface is given in terms of thickness (Angstroms) by an Inficon XTM/2 monitor. The deposition monitor has a resolution of 0.1 Å and rounds the deposition measurements to the nearest increment. To reduce fluctuations, averages were made over data points for the same deposition increment. On the scale of the plots, error bars are not much larger than the width of a moderately thick line, and therefore not shown.



Figures 3, 4, 5: Experiment compared to Theory for Cs on W for wavelengths of 407 nm, 532 nm, and 655 nm.

For the 407 nm case, Cs was deposited rapidly, so that the relationship between coverage and deposition depth was the diameter of the Cs atom ($\alpha = 0.52$ nm). For 532 and 655 nm, the deposition rate was slower so that Cs could desorb, making the relationship larger ($\alpha = 0.8$ nm). The location of the peak value is affected by residual Cs left on the W surface, and the presence of oxygen affects the work function variation. Therefore, to relate experiment to theory, we use

$$\theta(x) = \alpha(x_{\text{exp}} - x_{\text{max}}) + 63.537\% \quad [7]$$

where x is the experimental depth measurement, and 63.537% is the location of the minimum of $\Phi(\theta)$ for Cs on W as per GL theory. In the case of 655 nm, the photon energy is near the barrier maximum such that quantum mechanical reflection contributes. A crude model gives for the transmission coefficient that multiplies Eq. [2]

$$T_k = 4 \frac{\sqrt{(\hbar\omega + \mu)(\hbar\omega - \phi)}}{(\sqrt{\hbar\omega + \mu} + \sqrt{\hbar\omega - \phi})^2} \quad [8]$$

where ϕ is the height of the barrier above μ (e.g., in the case of Cs on W for 655 nm, it is 0.60). The experimental measurements are shown compared to the theory in Figures 3 through 5. The agreement is good. A comparison of all three side-by-side is shown in Figure 6.

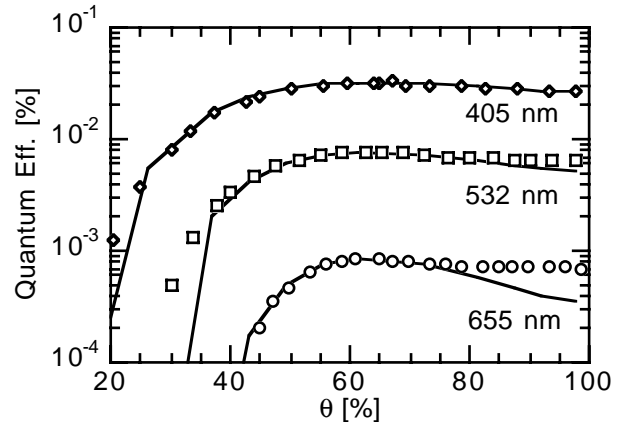


Figure 6: The data from Figures 3-5 on the same scale.

In spite of the dramatic reduction in work function caused by Cs on W, W nevertheless is not a good photoemitter material, and the resulting QE's are lower than needed. The cause is the scattering factor in QE is small because the electron scattering rates for W are so short that electrons are impeded in their attempts to escape after photoexcitation. The scattering factor for other metals is better, and, in the case of Ag, theory suggested that the quantum efficiency would be much better – perhaps not surprisingly given that Cs on Ag is a combination often found in photodetectors. Consequently, a recent experiment of the QE of Cs on Ag was performed. There are substantial differences in the values of parameters, like f , and the evaporation rates of Cs from Ag. Moreover, Ag is not as easily cleaned as W due to its much lower melting point. Finally, a detailed GL theory for Cs on Ag, though underway, is not yet

available. With those caveats, a comparison of theory with our recent experiments of the QE of Cs on Ag were made using the same (α) factor as for Cs on W. The results are shown in Figure 7, where, in spite of the evident differences (the theory is 3x larger and the spread is wider), the qualitative behavior of the theory is shown to be reasonable.

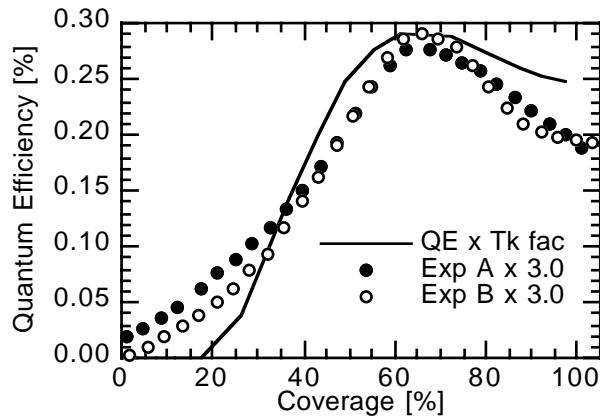


Figure 7: QE of Cs on Ag for 405 nm, under a field of 0.0174 MV/m. ϕ was chosen to give a minimum work function of 1.6 eV. Eq. [8] was found to be 0.81.

Part of the differences are presumably due to the non-optimal usage of the Cs-W parameters for the Cs-Ag configuration, but it is suspected that the factor of 3 discrepancy is based in large part to contamination of the surface and a reduction in effective photoemission area: Ag has a much lower melting point than W and therefore cannot be cleaned the same way. Support for this hypothesis is that adding a monolayer or more of oxygen (through exposure to high purity nitrous oxide for several minutes) to the Ag surface prior to cesiation does not increase the QE of Cs-Ag. If the original surface were indeed pure Ag, an increase in QE is expected due to dipole enhancement caused by the presence of oxygen. This observation suggests that surface contamination is present and therefore presumably responsible for the difference between the theory and experimental curves of Figure [7].

CONCLUSION

A photoemission model of a laser-heated cathode with a low work function coating gives excellent agreement with Cs on W experimental data. Agreement with longer-wavelength laser light was dependent upon the inclusion of a factor to account for quantum mechanical reflection of incident electrons at or near the barrier maximum. Initial Cs on Ag experimental data has qualitatively similar features: the theory is a factor of 3 larger due to, we have argued, contamination issues. We argue that a cesiated controlled porosity dispenser cathode therefore has promise, and the theoretical models can transition to beam simulation codes that require photoemission models.

Acknowledgements

We gratefully acknowledge funding provided by the *Joint Technology Office* and the *Office of Naval Research*. We have benefited from interactions with many colleagues, in particular, Joan Yater and Jonathan Shaw (NRL), David Dowell (SLAC), John Lewellen, Sandra Beidron, and Matt Virgo (ANL), Courtland Bohn (NIU), Dimitre Dimitrov (TechX), John Petillo (SAIC), and David Demske (UMD).

REFERENCES

- 1 P. G. O'Shea, H. Freund, *Science* **292**, 1853 (2001).
- 2 C. Travier, *Nucl. Inst. Meth.* **A304**, 285 (1991).
- 3 T. Srinivasan-Rao, J. Schill, I. Ben Zvi, M. Woodle, *Rev. Sci. Instrum.* **69**, 2292 (1998)
- 4 J. A. Nation, L. Schächter, F. M. Mako, L. K. Len, W. Peter, C.-M. Tang, T. Srinivasan-Rao, *Proceedings of the IEEE* **87**, 865 (1999).
- 5 K. L. Jensen, D. W. Feldman, M. Virgo, P. G. O'Shea, *Phys. Rev. Spec. Top.* **AB6**, 083501 (2003).
- 6 K. L. Jensen, D. W. Feldman, P. G. O'Shea, *Appl. Phys. Lett.* **85**, 5448 (2004).
- 7 C. Travier, B. Leblond, M. Bernard, J. N. Cayla, P. Thomas, P. Georges, *Proceedings of the Particle Accelerator Conference*, Dallas, TX, 1995, p. 945.
- 8 John Lewellen (ANL) (*private communication*).
- 9 D. Dimitrov, D. L. Bruhwiler, J. R. Cary, P. Messmer, P. Stoltz, D. Feldman, P. G. O'Shea, K. L. Jensen, "TPPE039—Development of Advanced Models for 3D Photocathode PIC Simulations" (*Particle Accelerator Conference*, Knoxville TN, 2005).
- 10 J. J. Petillo, E. M. Nelson, J. F. DeFord, N. J. Dionne, B. Levush, *IEEE Trans. El. Dev.* **52**, 742 (2005).
- 11 Courtland Bohn (NIU) (*private communication*).
- 12 K. L. Jensen, D. W. Feldman, P. G. O'Shea, *J. Vac. Sci. Technol.* **B23**, 621 (2005).
- 13 K. L. Jensen, D. W. Feldman, N. Moody, P. G. O'Shea, "A Photoemission Model For Low Work Function Coated Metal Surfaces And Its Experimental Validation" (submitted for publication)
- 14 T. Srinivasan-Rao, J. Fischer, T. Tsang, *J. Appl. Phys.* **69**, 3291, (1990).
- 15 D. Dowell (SLAC) (*private communication*).
- 16 E. P. Gyftopoulos, J. D. Levine, *J. Applied Physics* **33**, 67 (1962).
- 17 J. B. Taylor, I. Langmuir, *Phys. Rev.* **44**, 423 (1933); C-S Wang, *J. Appl. Phys.* **44**, 1477 (1977)